Article

Discovery Medicine 2025; 37(200): 1950–1960
https://doi.org/10.24976/Discov.Med.202537200.168

Effects of the BET Family Inhibitor JQ1 on Autophagy and Neuroprotection in Intracerebral Hemorrhage Rat Models: The Role of BRD4

Guo-qing Wang[1], Jia-jia Xia[2], Jie Sun[1], Jian-ying Shi[1], Li-jing Zhang[1], Ye-qiong Liu[1], Jie Liu[1], Yi-bing Peng[3,*]

[1]Clinical Laboratory Department, Jiading District Central Hospital Affiliated Shanghai University of Medicine & Health Sciences, 201800 Shanghai, China
[2]Nursing Department, Jiading District Central Hospital Affiliated Shanghai University of Medicine & Health Sciences, 201800 Shanghai, China
[3]Clinical Laboratory Department, Ruijin Hospital Affiliated Shanghai Jiao Tong University of Medicine, 200025 Shanghai, China
*Correspondence: pyb9861@sina.com (Yi-bing Peng)
Submitted: 16 July 2025 Revised: 11 August 2025 Accepted: 19 August 2025 Published: 20 September 2025

Background: Intracerebral hemorrhage (ICH) is a subtype of stroke causing severe neuronal injury and functional deficits. This study aims to investigate the impact of bromodomain-containing protein 4 (BRD4) on ICH progression and the therapeutic efficacy of the bromodomain and extraterminal (BET) inhibitor JQ1.

Methods: An ICH rat model was established by injecting autologous blood into the basal ganglia. During treatment, the rats received either JQ1 (50 mg/kg) or vehicle. Neurological and motor outcomes were measured via the foot-fault test, modified neurological severity score, and rotarod performance test. Cognitive function of the experimental rats was tested with the Morris water maze. Brain edema of the animals was evaluated using the wet–dry weight method, coupled with some histopathologic assessments by hematoxylin–eosin (H&E) staining, terminal deoxynucleotidyl transferase dUTP nick end labeling (TUNEL) assays were employed to analyze neuronal apoptosis. Expression of proteins related to apoptosis, autophagy, and the AMP-activated protein kinase/mammalian target of rapamycin (AMPK/mTOR) pathway were evaluated using Western blotting.

Results: BRD4 expression was notably increased in the cerebral tissue of ICH rats ($p < 0.01$), while the administration of JQ1 decreased the levels of BRD4 in rats with ICH ($p < 0.01$). The administration of JQ1 resulted in a reduction in the modified neurological severity score of ICH, a decrease in the misstep frequency of the left forelimb, and a longer time to slip ($p < 0.01$). Furthermore, relative to the ICH group, rats in the ICH + JQ1 group exhibited a reduction in escape latency, as well as increased platform crossings and longer durations in the target area ($p < 0.05$). Also, JQ1 reduced the water content, tissue damage, and apoptosis levels in the cerebral tissue affected by ICH ($p < 0.01$). The JQ1-induced reduction in BRD4 expression inhibited apoptosis-linked protein expression and promoted autophagy-associated protein expression ($p < 0.01$). Furthermore, JQ1 treatment elevated the p-AMPK/AMPK ratio and suppressed p-mTOR/mTOR levels ($p < 0.01$).

Conclusion: JQ1 holds the promise in alleviating ICH-induced brain injury by inhibiting BRD4 and modulating the AMPK/mTOR pathway.

Keywords: bromodomain-containing protein 4; JQ1; intracerebral hemorrhage; AMPK/mTOR pathway; autophagy

Introduction

Intracerebral hemorrhage (ICH) is a subtype of stroke characterized by non-traumatic bleeding within the cerebral tissue, frequently leading to high mortality and poor clinical outcomes [1]. ICH accounts for nearly 50% of stroke-related morbidity and mortality [2]. Additionally, ICH survivors may experience cognitive and motor impairment, facing substantial healthcare and financial burdens together with their families [3,4]. According to the statistical data from 2018, the global incidence of ICH was six cases per 100,000 people [4]. Alarmingly, the incidence of ICH continues to present a rising trajectory and has now emerged as a significant global health concern [5]. The ICH-induced brain injury is pathophysiologically complex. In essence, following ICH, rapid blood accumulation in the adjacent cerebral tissue can reportedly lead to increased intracranial pressure, edema, and neuroinflammation [6], subsequently triggering a cascade of secondary injuries that result in severe neural damage. Inflammation, oxidative stress, iron toxicity, apoptosis, autophagy, and other cellular biological processes have been identified as pivotal factors associated with ICH [7]. Advances in treatment modalities over the past few decades have contributed to the development of both surgical and medical strategies [8]. Nevertheless, the optimal timing for executing surgical interventions is still

unclear, and the efficacy of medications, such as statins, remains contentious [9], as existing treatments for addressing ICH-induced brain injury are not completely effective. Thus, this underscores the exigency of exploring and establishing new therapeutic approaches for ICH.

Patients with ICH mainly suffer from neuronal damage, inhibition of synaptic plasticity, and cognitive dysfunction. In the aftermath of ICH, significant damage occurs in the hippocampal Cornu Ammonis 1 (CA1) and Cornu Ammonis 3 (CA3) regions, with edema, inflammation, and perihematomal edema worsening neuronal injury [10]. Changes in synaptic activity become notably pronounced on day 7, with decreased synaptic potentials in the ipsilateral hippocampus and compensatory enhancement in the contralateral hippocampus, which are correlated with cognitive decline [11]. Increased histone deacetylase (HDAC) activity post-ICH reduces acetylation, inhibiting plasticity and further impairing cognition [12]. Additionally, mitochondrial dysfunction and ferroptosis contribute to neuronal loss and cognitive impairment [13]. Overall, ICH causes severe disruptions to hippocampal function and cognitive deficits.

Bromodomain-containing protein 4 (BRD4), belonging to the bromodomain and extraterminal (BET) protein family, functions as an epigenetic reader and contains two conserved N-terminal bromodomains (BD1 and BD2) and one extraterminal domain [14]. BRD4 is known to facilitate RNA polymerase II-mediated transcription by binding to acetylated lysine residues on histones and non-histone proteins, thereby regulating gene expression [15,16]. Genomic profiling has revealed widespread occupancy of BRD4 across active promoters, enhancers, and super-enhancers [17]. Due to its role in modulating gene expression, BRD4 is crucial for the regulation of embryonic patterning, cellular proliferation, immune responses, as well as metabolic processes [18]. BRD4 dysregulation is associated with various human diseases, including cancer, inflammatory disorders, and cardiovascular diseases such as heart failure, hypertension, and atherosclerosis [19–21]. However, research on the association between BRD4 and ICH remains relatively limited.

JQ1, is a potent and selective small-molecule inhibitor of BET proteins, especially BRD4. It acts by competitively binding to the acetyl-lysine recognition motif within the bromodomain, thereby disrupting the interaction between BRD4 and acetylated chromatin and suppressing downstream transcriptional activation [22]. Initially developed for cancer treatment, JQ1 has been shown to exert anti-inflammatory, anti-apoptotic, and neuroprotective effects in preclinical models of stroke, neurodegeneration, and traumatic brain injury [23,24]. In neural contexts, JQ1 has been reported to inhibit microglial activation, modulate autophagy, and suppress the expression of pro-inflammatory genes. Despite these promising findings, the role of JQ1 in ICH has not been systematically investigated. Given BRD4's regulatory function in inflammation and apoptosis—two key mechanisms of secondary brain injury after ICH—it is plausible that JQ1 may provide neuroprotective effects in this condition.

Hence, this work was designed to investigate the correlation between BRD4 and ICH and assess intervention effects of JQ1 on ICH through animal-based experiments.

Materials and Methods

Establishment ICH Rat Model

Forty Sprague–Dawley male rats (8–12 weeks, each weighing 250–300 g) were provided by Hunan Slack Jingda Experimental Animal Co., Ltd. (Hunan, China). The rats, certified to be free of specific pathogens, were deemed suitable for experimental research. The animals were kept under the following controlled conditions (22–24 °C, 50–60% humidity, 12-h light/dark schedule), with sterile food and water given ad libitum. All *in vivo* protocols were authorized by the Ethics Committee of Shanghai University of Medicine & Health Sciences (Approval Number: 2022-KY-08-16-341024198310280017). These protocols were in adherence to the ethical standards of the National Institutes of Health.

Consistent with previous studies, the ICH model was established through stereotactic infusion of autologous blood into the rat's basal ganglia [25]. First, the rats were fully anesthetized with isoflurane (1.5–2%) via spontaneous inhalation, then secured in a prone position onto the brain stereotaxic apparatus (71000, RWD, China). Next, a 1 mm craniotomy was performed to position the needle tip (26 gauge) at coordinates 3.2 mm lateral, 0.4 mm anterior and 5.8 mm deep. To establish an ICH model, 50 µL of fresh autologous whole blood was administered into the right striatum at a constant rate of 8 µL/minute. After 10 min, a second 50 µL volume was transfused to the same location at the same rate, bringing the total volume to 100 µL. Following the completion of the blood administration, the needle remained inserted for 10 min. Subsequently, the posterior needle was carefully withdrawn, and the incision was closed with sutures.

Experimental Grouping

A total of 40 rats were randomly allocated to four groups ($n = 10$ per group): (1) Sham group: Rats underwent only needle insertion without any blood injection and were administered 50 mg/kg solvent intraperitoneally. (2) JQ1 group: Rats received needle insertion without blood injection and were administered JQ1 intraperitoneally at a dose of 50 mg/kg, with daily dosing for three consecutive days. (3) ICH group: Rats were induced to develop ICH and then were given 50 mg/kg solvent. (4) ICH + JQ1 group: Rats were induced to develop ICH, as described, and were given 50 mg/kg of JQ1 intraperitoneally 2-h post-procedure, with daily dosing for three consecutive days.

The dosage and route of JQ1 administration were based on published studies that demonstrate its efficacy and safety in rodent models of neurological disorders and inflammation [14,26]. Furthermore, our preliminary experiments confirmed that this dosage was well tolerated in rats, with no observable adverse effects on behavior or major organs.

Modified Neurological Severity Score

The modified neurological severity score (mNSS) test was applied to systematically evaluate neurological deficits in rats after ICH induction. This comprehensive assessment included motor, sensory, reflex, and balance tests, with cumulative scores ranging from 0 (indicating no observable neurological deficits) to 18 (denoting severe neurological dysfunction). Neurological assessments were conducted before ICH induction and at designated intervals (24 h, 72 h, 7 d, and 14 d) post-ICH to capture both immediate and longer-term neurological changes. These tests included measuring the accuracy of forelimb placements, the responsiveness of sensory whiskers to external stimuli, the ability to regain an upright position from a supine posture, and the capacity to maintain balance under challenging conditions [27].

Foot-Fault Test

Foot-fault test was used to evaluate sensorimotor ability in spontaneous movements to identify gait disorders in each group of rats. The metal grid used measured 45 cm (length) × 45 cm (width) × 50 cm (height), with a cell size of 2.5 cm. The rats were placed at the center of the apparatus, and the left forelimb steps and foot faults were recorded for 1 min. Proportion of foot-fault steps was employed for statistical analysis. This test was conducted before modeling, and at 24/72 h, 7 d, and 14 d post-ICH.

Rotarod Performance Test

The rotarod performance test was employed to quantitatively assess locomotor function in rats post-ICH. The rotation velocity of Rotarod apparatus (ZH-300B, Zhenghua Biological Equipment, Co., Ltd., Anhui, China) was increased steadily from 5 rpm to 35 rpm in 60 s with a 0.5 rpm adjustment per second. Duration the animals spent on the rod was measured. The mean of the recorded durations for three consecutive runs each day was measured. Testing was conducted before modeling and at 24/72 h, 7 d, and 14 d post-ICH.

Morris Water Maze Test

All experimental rats were assessed for spatial navigation deficits using the Morris water maze. The rats were evaluated from days 21 to 25 after ICH induction in a circular pool (diameter: 180 cm, depth: 50 cm). A transparent 20 cm platform was positioned 2 cm below water level. Data for escape latency, swim path, distance to the hidden platform, and velocity were collected using the Morris water maze video-tracking system (RD1101-MWM-G, Mobile Datum, China). The spatial probe test, with the hidden platform removed, was conducted before modeling and at 24/72 h, 7 d, and 14 d post-ICH, to measure the time spent by each rat traversing the former platform quadrant.

Measurement of Brain Water Content

After undergoing a series of the behavioral and neurological assessments, the rats were humanely euthanized with 2% sodium pentobarbital (120 mg/kg) 14 days after ICH induction. The wet–dry weight approach was applied to determine brain water content in the Sham, JQ1, ICH, and ICH + JQ1 groups after treatment. The dry and wet weight techniques involved weighing the excised cerebral tissue immediately after removal (wet weight), drying it in an oven at 100 °C for 24 h, and then re-weighing it (dry weight). The brain water content was calculated using the formula below:

Brain water content (%) = (Wet weight – Dry weight)/Wet weight × 100.

TUNEL Assay

Neuronal apoptosis in cerebral tissue was evaluated using the terminal deoxynucleotidyl transferase dUTP nick end labeling (TUNEL) assay. Briefly, cerebral slices were treated with TUNEL solution available in the *in-situ* Cell Death Detection Kit, TMR red (Roche, Basel, Switzerland), and the nucleus was stained with 4',6-diamidino-2-phenylindole (DAPI). Then, TUNEL-positive cells were enumerated under a Nikon Ni microscope (Nikon, Tokyo, Japan) by an investigator who was blinded to the study design. The target regions in the ipsilateral hemisphere were located around the hematoma, with the needle insertion site excluded. The analysis results were expressed as a percentage of TUNEL-positive cells.

Hematoxylin–Eosin Staining

Following immersion-fixation in a 4% formaldehyde solution for 1 to 7 days, the cerebral samples were processed in an automated tissue-processing unit (STP-120, Thermo Fisher Scientific, UK). Subsequently, the tissues were paraffin-embedded and sectioned coronally at thicknesses of 3 and 5 µm using a microtome (HM 325, Thermo Fisher Scientific, China). Tissue sections were then subjected to xylene dewaxing, followed by rehydration through a series of graded ethanol solutions and deionized water, prior to histological staining. Specifically, 3-µm-thick sections were stained with hematoxylin–eosin (H&E) according to the established protocols, and the stained sections were then photographed under a BX43 Olympus microscope (Olympus Corporation, Tokyo, Japan).

Western Blotting

Cerebral tissue samples surrounding the hematoma sites were disrupted, homogenized, and lysed in chilled radio-immunoprecipitation assay (RIPA) lysis buffer (Boster, AR0105-100) for 30 min. Protein concentration was determined using a BCA protein assay kit following the manufacturer's instructions. Equal amounts of protein (20 µg) were separated by 10% SDS-PAGE and the separated bands were subsequently transferred to PVDF membranes. Next, PVDF membrane was blocked using 5% skim milk for 2 h at ambient temperature, followed by incubation with primary antibodies overnight at 4 °C. Antibodies targeting BRD4 (A18840, Abclonal, 1:1000), Bcl-2 (A21592, Abclonal, 1:1000), BAX (A19684, Abclonal, 1:1000), cleaved caspase-1 (4199, CST, 1:1000), LC3-I (4599, CST, 1:1000), LC3-II (2775, CST, 1:1000), p62 (A7758, Abclonal, 1:1000), Beclin (Becn1, A7353, Abclonal, 1:1000), AMPK (A1229, Abclonal, 1:1000), phosphorylated AMPK (AP0871, Abclonal, 1:1000), mTOR (A2445, Abclonal, 1:1000), phosphorylated mTOR (AP0115, Abclonal, 1:1000), and GAPDH (AC002, Abclonal, 1:15,000) were utilized in this experiment. After washing, membranes were incubated for 1 h at ambient temperature with HRP-conjugated secondary antibodies, including goat anti-rabbit IgG (AS014, Abclonal, 1:5000) or goat anti-mouse IgG (AS003, Abclonal, 1:5000). Afterwards, protein visualization was achieved with an ECL detection kit (Thermo Fisher Scientific, MA, USA) and quantified using ImageJ software v1.53 (NIH, Bethesda, MD, USA).

Statistical Analysis

Statistical analysis was carried out using SPSS v26.0 (IBM Corp., Armonk, NY, USA). Prior to group comparisons, the Shapiro–Wilk test was applied to evaluate the normality of data distribution. For variables conforming to a normal distribution, results are expressed as mean ± standard deviation (SD), and differences among groups were assessed using one-way analysis of variance (ANOVA) with Tukey's post hoc test. For datasets that did not meet the normality assumptions, data are presented as median and interquartile range (IQR), and Kruskal–Wallis test, followed by Dunn's post hoc test, was used. Results with $p < 0.05$ were considered statistically significant.

Results

Intracerebral Hemorrhage Elevates the Expression of BRD4

To investigate the temporal expression profile of BRD4 after ICH, we measured BRD4 protein levels in perihematomal brain tissue at 12 h, 24 h, 72 h, and 7 days post-ICH. The results showed that the levels of BRD4 protein increased gradually at 12/24/72 h post-ICH ($p < 0.01$), but decreased significantly at 7 days ($p < 0.01$) (Fig. 1A,B). This dynamic pattern suggested that BRD4 was actively involved in the acute phase of ICH and might participate in the subsequent secondary injury processes.

JQ1 Mitigates Cerebral Edema and Damage in ICH

JQ1 is considered a highly effective suppressor of BRD4 expression and is commonly utilized in cancer research [28]. In this study, JQ1 was used to examine the impact of BRD4 suppression on the brain in an ICH model. In the assessment of JQ1's inhibitory effect, the BRD4 expression was notably reduced in the ICH + JQ1 group ($p < 0.01$) (Fig. 2A,B). Unsurprisingly, the brain water content for the ICH + JQ1 group showed a marked reduction relative to the ICH group ($p < 0.01$) (Fig. 2C). Furthermore, H&E staining revealed anomalies in the cerebral tissue of the ICH rat model, featuring neuronal swelling, necrosis of certain nerve cells, atrophy, deformation, nuclear condensation, nuclear fragmentation, and inflammatory cell infiltration. However, these features were ameliorated following the administration of JQ1, characterized by a reduction in the morphological alterations of cerebral tissue, the number of necrotic nerve cells, and inflammatory cell infiltration (Fig. 2D). Collectively, these findings corroborated the potential of JQ1 in alleviating post-ICH brain tissue damage.

JQ1 Attenuates Neurological and Motor Deficits Induced by ICH

Cognitive and motor impairments are common manifestations of ICH [29]. In this study, a series of behavioral assessments was conducted upon the injection of JQ1 in ICH rats. The assessment outcomes revealed a substantial decrease in mNSS in the ICH + JQ1 group relative to the ICH group at 24 h, 72 h, and 7 d post-ICH induction ($p < 0.01$). However, this difference was not statistically significant at day 14 post-ICH, which may be attributed to the limited duration of JQ1 administration or the recovery plateau commonly observed in later stages of ICH (Fig. 3A). In contrast, the ICH + JQ1 group exhibited a decreased foot fault rate and increased latency on the rotarod performance test relative to the ICH group ($p < 0.05$ or $p < 0.01$) (Fig. 3B,C). The aforementioned findings indicated that the JQ1 treatment significantly alleviated neurological damage and behavioral abnormalities in the ICH model.

JQ1 Attenuates Learning and Memory Impairments Caused by ICH

Subsequently, we assessed the cognitive and memory abilities in rats of each group through the Morris water maze. The assessment outcomes demonstrated that escape latency was greatly reduced in the ICH + JQ1 group versus the ICH group ($p < 0.01$) (Fig. 4A). Additionally, compared to the ICH group, the ICH + JQ1 group exhibited a notable elevation in the platform-crossing frequency and target-quadrant dwelling time ($p < 0.05$ or $p < 0.01$)

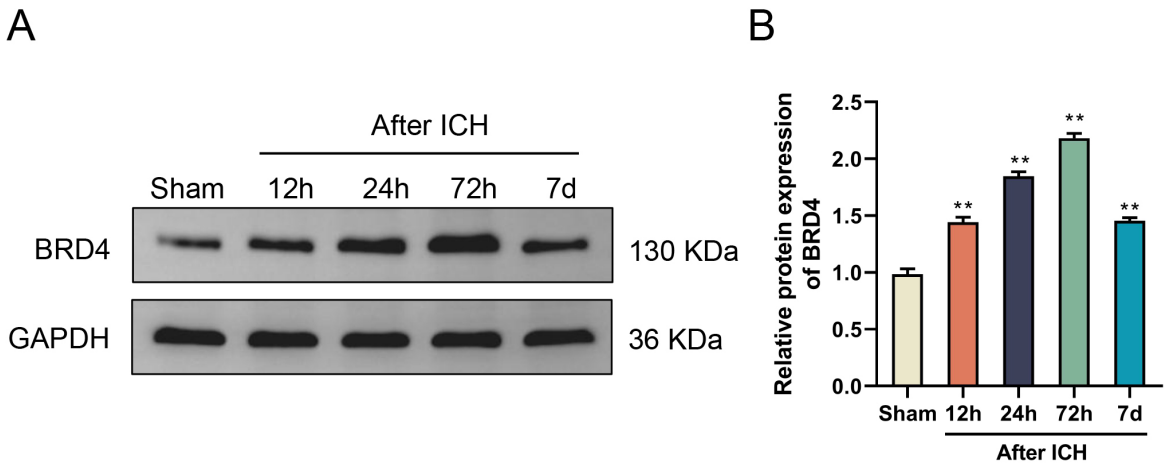

Fig. 1. Intracerebral hemorrhage elevates BRD4 expression. (A) Western blot analysis of BRD4 protein expression. (B) Quantitative results of the BRD4 protein expression, presented as mean ± SD (n = 3). **$p < 0.01$ vs. Sham group. Abbreviations: BRD4, bromodomain-containing protein 4; ICH, intracerebral hemorrhage.

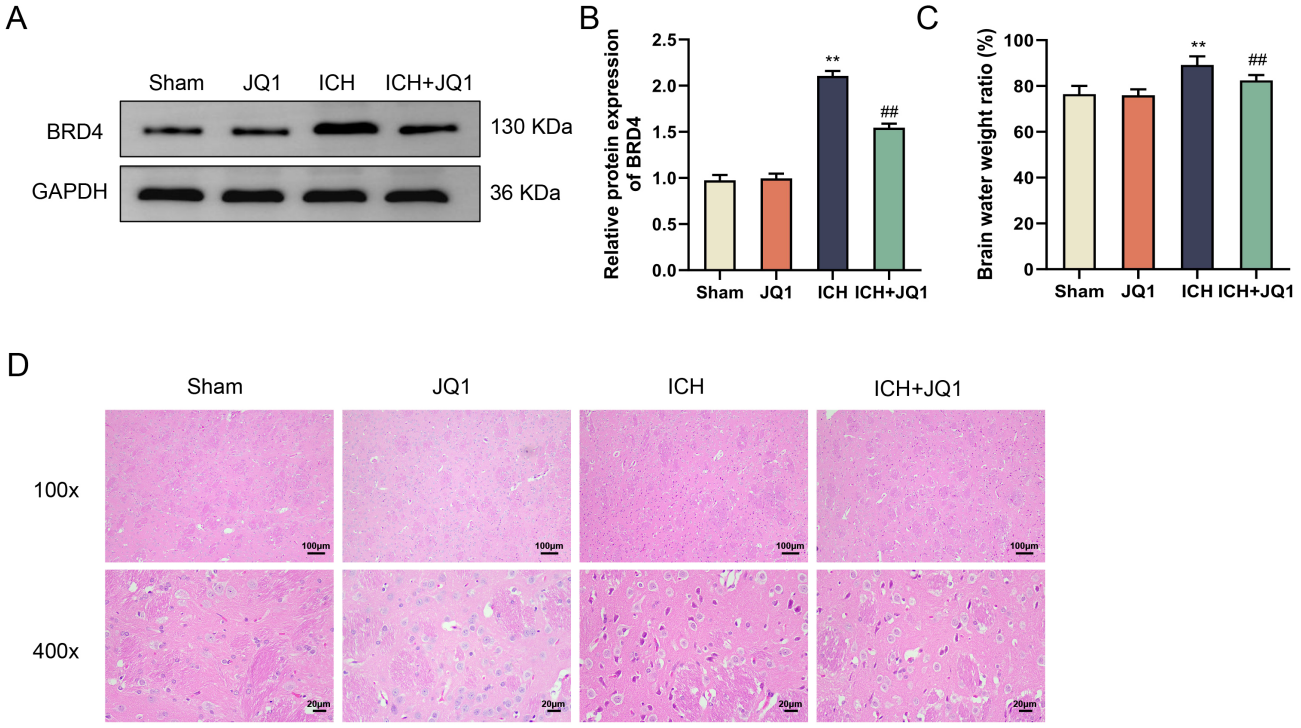

Fig. 2. JQ1 mitigates cerebral edema and damage in ICH. (A) Western blot analysis of BRD4 protein. (B) Quantitative results of the BRD4 protein expression. (C) Brain water content (n = 10). (D) H&E staining (scale bars: 100 μm or 20 μm). Quantitative results are presented as mean ± SD (n = 3). **$p < 0.01$ vs. Sham group; $^{\#\#}p < 0.01$ vs. ICH group. Abbreviations: BRD4, bromodomain-containing protein 4; ICH, intracerebral hemorrhage; H&E, hematoxylin–eosin.

(Fig. 4B,C). These observations indicated that JQ1 administration could attenuate learning and memory impairments after ICH.

JQ1 Alleviates Apoptosis in Cerebral Tissue Induced by ICH

Apoptosis induced by ICH is a contributing factor to brain dysfunction and the onset of stroke [30]. In this study, TUNEL assay was employed for examining apoptosis within different regions of the experimental rats' cerebral tissues. The staining results showed a notable suppression of apoptosis in cerebral tissues of ICH rats following JQ1 administration, as compared to the untreated ICH rats ($p < 0.01$) (Fig. 5A,B). Subsequently, the levels of proteins associated with apoptosis were evaluated. According to the evaluation results, the ICH + JQ1 group exhibited a

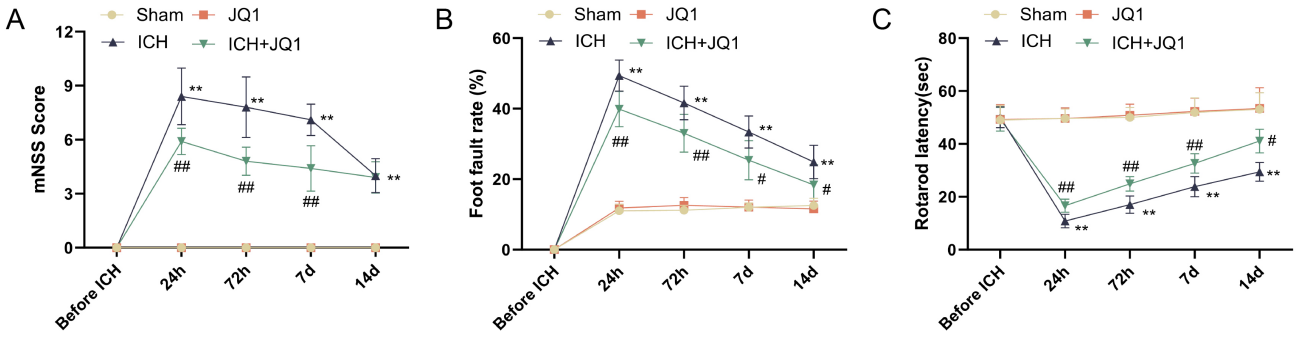

Fig. 3. JQ1 alleviates neurological and motor deficits induced by ICH. (A) mNSS score. (B) Foot fault rate. (C) Rotarod latency. Results are presented as median (IQR) ($n = 10$). **$p < 0.01$ vs. Sham group; $^{\#}p < 0.05$, $^{\#\#}p < 0.01$ vs. ICH group. Abbreviations: mNSS, modified neurological severity score; ICH, intracerebral hemorrhage.

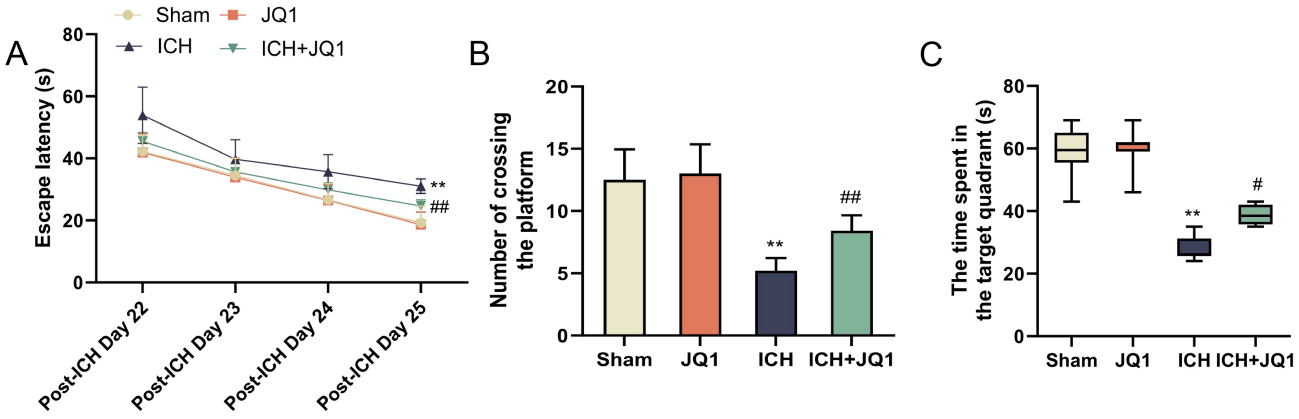

Fig. 4. JQ1 attenuates learning and memory impairments caused by ICH. (A) Escape latency. (B) Number of platform-crossing. (C) Target-quadrant dwelling time. These variables were measured by means of Morris water maze test. Results are reported as mean ± SD ($n = 10$). **$p < 0.01$ vs. Sham group; $^{\#}p < 0.05$, $^{\#\#}p < 0.01$ vs. ICH group. Abbreviation: ICH, intracerebral hemorrhage.

marked elevation in Bcl-2 protein expression and a notable reduction in BAX and cleaved caspase-1 relative to the ICH group ($p < 0.01$) (Fig. 5C,D). These observations suggested that JQ1 could suppress cell apoptosis induced by ICH.

JQ1 Activates Autophagy in Cerebral Tissues of ICH Rats

According to an earlier study, promoting autophagy is beneficial for the treatment of neurological disorders [31]. In this study, Western blotting was employed to examine expression of autophagy-related proteins in the cerebral tissues of different groups of rats. The LC3-II and Beclin-1 levels in the ICH + JQ1 group were considerably upregulated in contrast to the ICH group, whereas the p62 protein levels were remarkably reduced ($p < 0.01$) (Fig. 6A,B). These results suggested that JQ1 might play a role in improving the condition of cerebral tissues in ICH rats by modulating autophagy pathway.

JQ1 Regulates the AMPK/mTOR Pathway

The activation of mTOR (p-mTOR) is an inhibitory signal for autophagy. In this study, compared to the Sham group, p-AMPK/AMPK levels were notably elevated in ICH rats, while p-mTOR/mTOR levels were substantially decreased. However, there was a notable reduction in p-mTOR/mTOR levels and an obvious elevation in p-AMPK/AMPK levels within the ICH + JQ1 group ($p < 0.01$) (Fig. 7A,B). These findings suggested that JQ1 might influence autophagy via AMPK/mTOR signaling.

Discussion

Intracerebral hemorrhage may lead to mobility limitations, cognitive decline, and mortality, posing a significant risk to human health and well-being [32]. At the current stage, the therapeutic benefits and long-term prospects of surgical intervention are relatively limited, and the efficacy of medications is constrained by their adverse effects [33]. Thus, identifying new therapeutic targets and effective neuroprotective strategies remains a pressing need. In our study, JQ1 showed potential as a promising intervention for the treatment of ICH.

This study revealed that after ICH induction in rats, BRD4 expression progressively increased from 12 h to 72

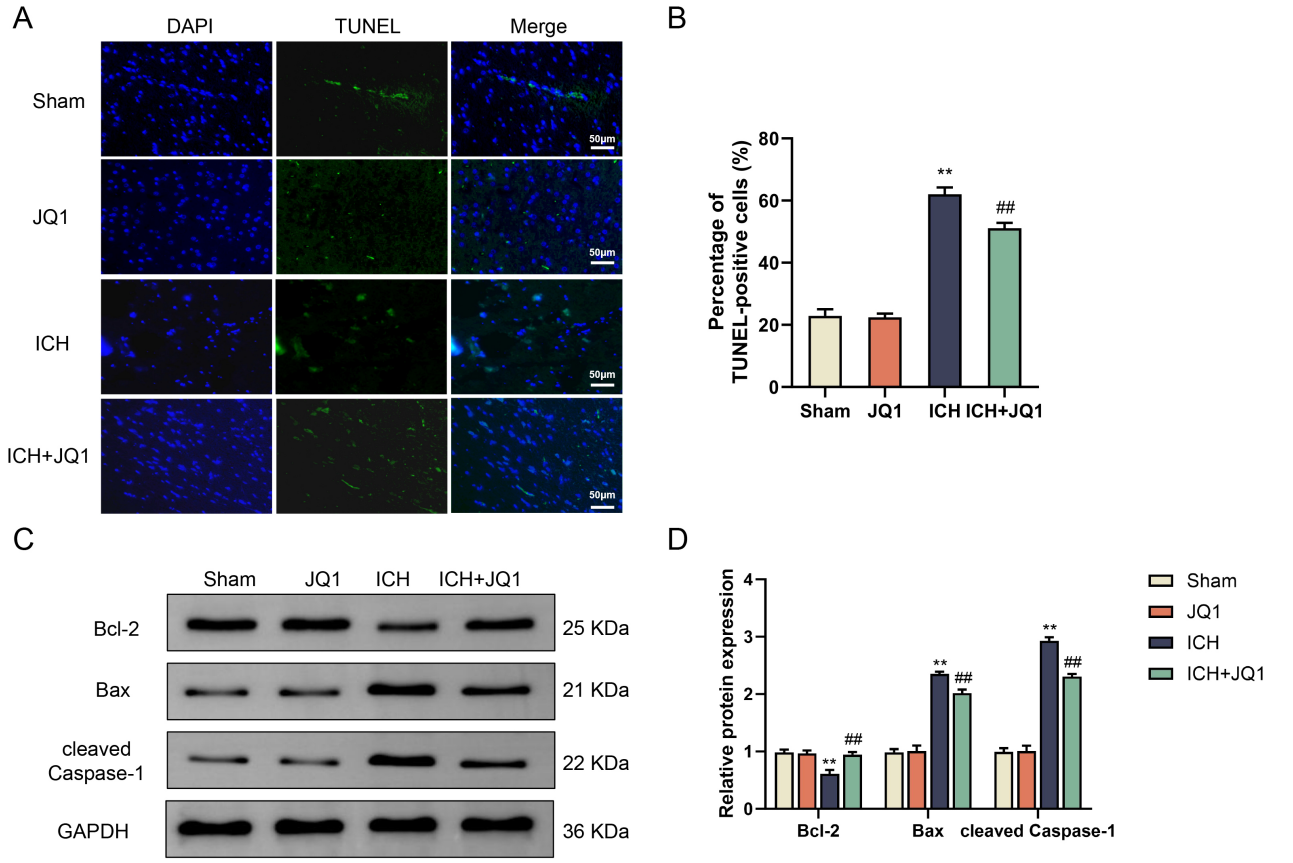

Fig. 5. JQ1 alleviates apoptosis in cerebral tissue of ICH rats. (A,B) TUNEL staining results (scale bar = 50 μm) and the corresponding quantitative analysis. (C) Western blots of Bcl-2, BAX, and cleaved caspase-1. (D) Quantitative analysis of the protein expression of Bcl-2, BAX, and cleaved caspase-1. Quantitative results are reported as mean ± SD ($n = 3$). $^{**}p < 0.01$ vs. Sham group; $^{\#\#}p < 0.01$ vs. ICH group. Abbreviation: ICH, intracerebral hemorrhage; TUNEL, terminal deoxynucleotidyl transferase dUTP nick end labeling.

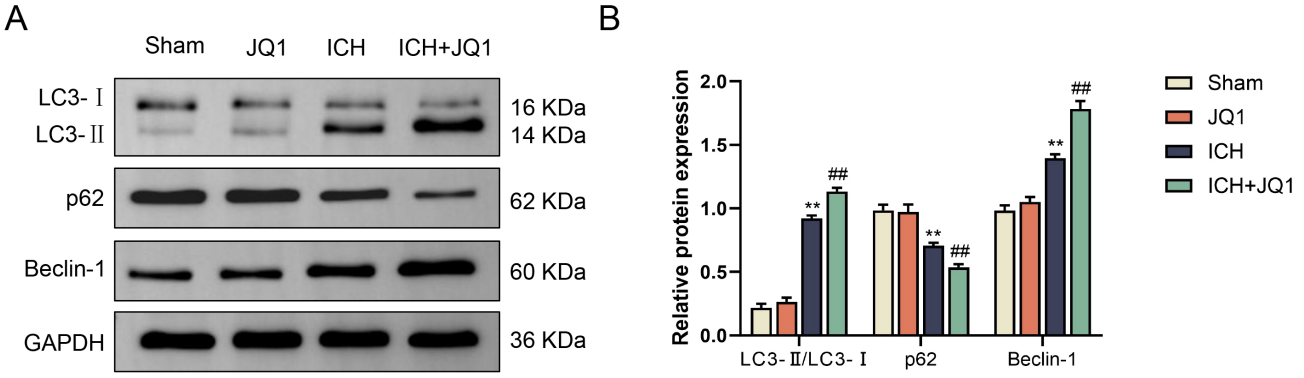

Fig. 6. JQ1 activates autophagy levels in the cerebral tissue of ICH rats. (A) Western blot analysis of LC3-I, LC3-II, p62, and Beclin-1. (B) Quantitative analysis of the protein expression of LC3-I, LC3-II, p62, and Beclin-1. Results are reported as mean ± SD ($n = 3$). $^{**}p < 0.01$ vs. Sham group; $^{\#\#}p < 0.01$ vs. ICH group. Abbreviation: ICH, intracerebral hemorrhage.

h, peaking at 72 h. Interestingly, the BRD4 expression level gradually decreased between 72 h and 7 days post-ICH induction. Additionally, it has been reported that primary injury induced by ICH occurs within minutes to hours following the onset of bleeding and is predominantly attributed to mechanical trauma caused by mass effect [34]. Secondary damage primarily occurs due to oxidative stress, intraparenchymal hemorrhage, cytotoxic effects due to rapid blood accumulation, and inflammatory responses, resulting in irreversible damage within the components comprising the neurovascular unit [35]. In view of previous studies, the upregulation of BRD4 expression is associated with the

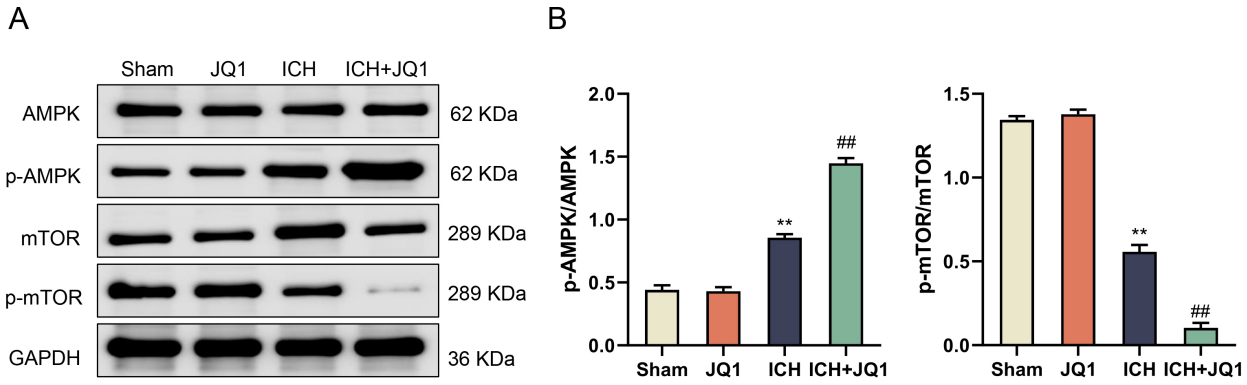

Fig. 7. JQ1 induces autophagy by regulating AMPK/mTOR signaling. (A) Western blot analysis of AMPK, p-AMPK, mTOR, and p-mTOR. (B) Quantitative analysis of the protein expression of AMPK, p-AMPK, mTOR, and p-mTOR. Results are reported as mean ± SD ($n = 3$). $^{**}p < 0.01$ vs. Sham group; $^{\#\#}p < 0.01$ vs. ICH group. Abbreviation: ICH, intracerebral hemorrhage; AMPK/mTOR, AMP-activated protein kinase/mammalian target of rapamycin.

progression of brain injury caused by ICH. Although a direct correlation between BRD4 and ICH-induced brain injury severity was not established within this study, it is still plausible to suggest that BRD4 could be significantly linked to brain injury caused by ICH.

JQ1, a highly potent small-molecule inhibitor of BET family members, blocks the recruitment of BRD4 to acetylated chromatin via competitive binding to its bromodomain motifs [36]. JQ1 has been reported to potently inhibit solid tumor growth [37,38]. For instance, Li *et al*. [26] reported that BET inhibition promoted neuronal differentiation and suppressed glial proliferation in neural progenitor cells, indicating a possible therapeutic role in neurodegeneration. The involvement of JQ1 in ICH has not been documented. This study revealed a notable decrease in BRD4 expression following the administration of JQ1 in the ICH model. Subsequent examinations demonstrated that the downregulation of BRD4 induced by JQ1 reduced brain water content and improved pathological manifestations in cerebral tissues after ICH, while also mitigating behavioral abnormalities, as well as learning and memory impairments in ICH. These findings suggested that JQ1-mediated inhibition of BRD4 expression might mitigate ICH-induced brain injury.

In numerous chronic neurodegenerative conditions, cell death is a major contributor to functional decline, and ICH-induced neuronal apoptosis could exacerbate brain injury [39]. Most recent experimental investigations have focused on elucidating the mechanism of neuronal apoptosis induced by ICH, aiming to identify novel therapeutic targets for this disease [40]. In an oncological study, specific inhibition of BRD4 has been demonstrated to trigger programmed cell death in diverse types of cancer cells [26]. However, in a study on acute kidney injury, BRD4 inhibition notably reduced the production of proteins associated with programmed cell death in renal tissue [41]. Similarly, JQ1 has been identified as an agonist of apoptosis in a cancer-related study [42]. In this study, notably elevated apoptosis rate was observed in cerebral tissues of ICH rats. However, JQ1-induced reduction in BRD4 expression led to a decreased level of apoptosis. Additionally, JQ1 was found to elevate Bcl-2 protein expression and decrease BAX and cleaved caspase-1 protein levels. These results indicate that BRD4 is an activating factor of neuronal apoptosis in ICH, which can be counteracted by JQ1.

Autophagy is a cellular protective mechanism through which cells break down and process misfolded proteins, injured organelles, intracellular pathogens, and various abnormal cell constituents [43]. Impaired autophagy can compromise cellular function and is strongly associated with neurodegenerative disorders [44]. BRD4 has been shown to inhibit the assembly of autophagosomes [45]. Besides, BRD4 inhibition leads to the activation of autophagy by upregulating various autophagy and lysosomal genes [46]. In addition, JQ1 can facilitate macrophage autophagy through the mTOR signaling pathway, thereby inhibiting the intracellular replication of HIV [47]. In this study, JQ1 markedly increased the autophagy levels in ICH cerebral tissue, potentially via the AMPK-mTOR pathway. Future research could explore the potential efficacy of mTOR inhibitors in ameliorating brain injury caused by ICH and further investigate the specific mechanisms by which JQ1 affects autophagy.

Importantly, increasing evidence indicates that apoptosis and autophagy are interconnected processes with mutual regulatory roles [48]. Autophagy can function as a compensatory survival mechanism that delays or suppresses apoptosis under stress conditions [49]. The current study found that JQ1 mediates concurrent reduction of apoptotic markers and stimulation of autophagy, which may be functionally linked, and that enhanced autophagy might contribute to the observed anti-apoptotic effects. This interplay warrants further mechanistic investigation in the context of ICH.

Although this research offers important perspectives on the neuroprotective function of JQ1 in rat ICH models, certain limitations must be acknowledged. First, JQ1 is a non-specific BET inhibitor. Due to JQ1's effects on other BET family proteins, it is difficult to conclusively attribute the observed neuroprotective effects solely to BRD4. Future research incorporating genetic approaches—such as siRNA-mediated knockdown or CRISPR-based editing—would help elucidate the precise contribution of BRD4 to ICH pathophysiology. In addition, this study was limited to a single animal model, and the absence of long-term outcome data raises concerns about the sustained efficacy and safety of BET inhibition. Furthermore, our research relied on H&E staining, which, although useful for general histological examination, lacks specificity to discern subtle types of neuronal injuries. Future studies should incorporate immunohistochemical markers such as glial fibrillary acidic protein (GFAP) and ionized calcium-binding adapter molecule 1 (IBA-1) to better characterize astrocyte and microglial activation during ICH progression and recovery. Additionally, we acknowledge the lack of lesion volume analysis, which is critical for evaluating both tissue damage and the protective effects of JQ1. We plan to include this analysis in future studies to offer a broader appraisal of JQ1's neuroprotective efficacy for treating intracerebral hemorrhage.

This study highlights the neuroprotective potential of JQ1 in ICH, but its broader application in other neurodegenerative diseases, where neuroinflammation plays a key role, should also be considered. JQ1 could complement existing treatments, and its non-specific BET inhibition suggests that it may work synergistically with other therapies. Therefore, future studies should refine these findings by using more specific inhibitors to clarify the role of BRD4 in neuroprotection. Expanding research to include models that more closely mimic human physiology and conducting long-term assessments will help understand the long-term effects and safety of BET inhibition. Additionally, integrating advanced histological techniques will help provide deeper insights into the cellular mechanisms involved in ICH recovery and neuronal damage, further improving treatment strategies.

Conclusion

Overall, the BRD4 inhibitor JQ1 can improve ICH-induced behavioral function, learning and memory impairments, as well as brain injury and cell apoptosis in the cerebral tissue of rats with the disorder. Furthermore, JQ1 can activate autophagy in the cerebral tissue of ICH rats. These effects may be mediated through the AMPK/mTOR cascade. This research reveals that BRD4 could serve as a promising therapeutic target in ICH management, and that JQ1 is a potential candidate for drug development for this disorder.

Availability of Data and Materials

The data used to support the findings of this study are available from the corresponding author upon request.

Author Contributions

GQW and YBP conceived and designed the study. JJX, JYS, and JL performed the experiments and data collection. JS, YQL, and LJZ contributed to data analysis, software application, and validation. JJX and LJZ were responsible for data curation and visualization. GQW and YBP drafted the manuscript. All authors reviewed the manuscript critically for important intellectual content, approved the final version, and agreed to be accountable for all aspects of the work in ensuring the accuracy and integrity of the study.

Ethics Approval and Consent to Participate

The study was reviewed and approved by the institutional review board of Shanghai University of Medicine & Health Sciences (Approval Number: 2022-KY-08-16-341024198310280017) and conducted in accordance with the ethical standards of the National Institutes of Health.

Acknowledgment

Not applicable.

Funding

This research received no external funding.

Conflict of Interest

The authors declare no conflict of interest.

References

[1] GBD 2019 Diseases and Injuries Collaborators. Global burden of 369 diseases and injuries in 204 countries and territories, 1990-2019: a systematic analysis for the Global Burden of Disease Study 2019. Lancet. 2020; 396: 1204–1222. https://doi.org/10.1016/S0140-6736(20)30925-9.

[2] Xue M, Yong VW. Neuroinflammation in intracerebral haemorrhage: immunotherapies with potential for translation. The Lancet. Neurology. 2020; 19: 1023–1032. https://doi.org/10.1016/S1474-4422(20)30364-1.

[3] Wang J, Wang T, Fang M, Wang Z, Xu W, Teng B, *et al*. Advances of nanotechnology for intracerebral hemorrhage therapy. Frontiers in Bioengineering and Biotechnology. 2023; 11: 1265153. https://doi.org/10.3389/fbioe.2023.1265153.

[4] Wilkinson DA, Pandey AS, Thompson BG, Keep RF, Hua Y, Xi G. Injury mechanisms in acute intracerebral hemorrhage. Neuropharmacology. 2018; 134: 240–248. https://doi.org/10.1016/j.neuropharm.2017.09.033.

[5] Bai C, Hao X, Zhou L, Sun Y, Song L, Wang F, *et al*. Machine learning-based identification of the novel circRNAs circERBB2 and circCHST12 as potential biomarkers of intracerebral hem-

orrhage. Frontiers in Neuroscience. 2022; 16: 1002590. https://doi.org/10.3389/fnins.2022.1002590.

[6] Wu L, Zhan Q, Liu P, Zheng H, Liu M, Min J, *et al*. LncRNA TCONS_00145741 Knockdown Prevents Thrombin-Induced M1 Differentiation of Microglia in Intracerebral Hemorrhage by Enhancing the Interaction Between DUSP6 and JNK. Frontiers in Cell and Developmental Biology. 2022; 9: 684842. https://doi.org/10.3389/fcell.2021.684842.

[7] Xie B, Qiao M, Xuan J. lncRNA MEG3 Downregulation Relieves Intracerebral Hemorrhage by Inhibiting Oxidative Stress and Inflammation in an miR-181b-Dependent Manner. Medical Science Monitor. 2021; 27: e929435. https://doi.org/10.12659/MSM.929435.

[8] Hostettler IC, Seiffge DJ, Werring DJ. Intracerebral hemorrhage: an update on diagnosis and treatment. Expert Review of Neurotherapeutics. 2019; 19: 679–694. https://doi.org/10.1080/14737175.2019.1623671.

[9] Wang X, Dong Y, Qi X, Huang C, Hou L. Cholesterol levels and risk of hemorrhagic stroke: a systematic review and meta-analysis. Stroke. 2013; 44: 1833–1839. https://doi.org/10.1161/STROKEAHA.113.001326.

[10] Wang KW, Liang CL, Yeh LR, Liu KY, Chen CC, Chen JS, *et al*. Simvastatin-Ezetimibe enhances growth factor expression and attenuates neuron loss in the hippocampus in a model of intracerebral hemorrhage. Fundamental & Clinical Pharmacology. 2021; 35: 634–644. https://doi.org/10.1111/fcp.12635.

[11] Shirzad S, Tayaranian Marvian M, Abroumand Gholami A, Ghrehbaghi M, Marefati N, Salmani H, *et al*. Unveiling the Effects of Left Hemispheric Intracerebral Hemorrhage on Long-term Potentiation and Inflammation in the Bilateral Hippocampus: A Preclinical Study. Journal of Stroke and Cerebrovascular Diseases. 2024; 33: 107523. https://doi.org/10.1016/j.jstrokecerebrovasdis.2023.107523.

[12] Okamura M, Inoue T, Takamatsu Y, Maejima H. Pharmacological inhibition of histone deacetylases ameliorates cognitive impairment after intracerebral hemorrhage with epigenetic alteration in the hippocampus. Journal of Stroke and Cerebrovascular Diseases. 2023; 32: 107275. https://doi.org/10.1016/j.jstrokecerebrovasdis.2023.107275.

[13] Li XN, Lin L, Li XW, Zhu Q, Xie ZY, Hu YZ, *et al*. BSA-stabilized selenium nanoparticles ameliorate intracerebral hemorrhage's-like pathology by inhibiting ferroptosis-mediated neurotoxicology via Nrf2/GPX4 axis activation. Redox Biology. 2024; 75: 103268. https://doi.org/10.1016/j.redox.2024.103268.

[14] Shi J, Vakoc CR. The mechanisms behind the therapeutic activity of BET bromodomain inhibition. Molecular Cell. 2014; 54: 728–736. https://doi.org/10.1016/j.molcel.2014.05.016.

[15] Donati B, Lorenzini E, Ciarrocchi A. BRD4 and Cancer: going beyond transcriptional regulation. Molecular Cancer. 2018; 17: 164. https://doi.org/10.1186/s12943-018-0915-9.

[16] Hu J, Pan D, Li G, Chen K, Hu X. Regulation of programmed cell death by Brd4. Cell Death & Disease. 2022; 13: 1059. https://doi.org/10.1038/s41419-022-05505-1.

[17] Altendorfer E, Mochalova Y, Mayer A. BRD4: a general regulator of transcription elongation. Transcription. 2022; 13: 70–81. https://doi.org/10.1080/21541264.2022.2108302.

[18] Andrieu GP, Shafran JS, Deeney JT, Bharadwaj KR, Rangarajan A, Denis GV. BET proteins in abnormal metabolism, inflammation, and the breast cancer microenvironment. Journal of Leukocyte Biology. 2018; 104: 265–274. https://doi.org/10.1002/JLB.5RI0917-380RR.

[19] Lu L, Chen Z, Lin X, Tian L, Su Q, An P, *et al*. Inhibition of BRD4 suppresses the malignancy of breast cancer cells via regulation of Snail. Cell Death and Differentiation. 2020; 27: 255–268. https://doi.org/10.1038/s41418-019-0353-2.

[20] Lin S, Du L. The therapeutic potential of BRD4 in cardiovascular disease. Hypertension Research. 2020; 43: 1006–1014. https://doi.org/10.1038/s41440-020-0459-4.

[21] Yang YM, Shi RH, Xu CX, Li L. BRD4 expression in patients with essential hypertension and its effect on blood pressure in spontaneously hypertensive rats. Journal of the American Society of Hypertension. 2018; 12: e107–e117. https://doi.org/10.1016/j.jash.2018.11.004.

[22] Pang Y, Bai G, Zhao J, Wei X, Li R, Li J, *et al*. The BRD4 inhibitor JQ1 suppresses tumor growth by reducing c-Myc expression in endometrial cancer. Journal of Translational Medicine. 2022; 20: 336. https://doi.org/10.1186/s12967-022-03545-x.

[23] Zhou Y, Gu Y, Liu J. BRD4 suppression alleviates cerebral ischemia-induced brain injury by blocking glial activation via the inhibition of inflammatory response and pyroptosis. Biochemical and Biophysical Research Communications. 2019; 519: 481–488. https://doi.org/10.1016/j.bbrc.2019.07.097.

[24] Li Y, Xiang J, Zhang J, Lin J, Wu Y, Wang X. Inhibition of Brd4 by JQ1 Promotes Functional Recovery From Spinal Cord Injury by Activating Autophagy. Frontiers in Cellular Neuroscience. 2020; 14: 555591. https://doi.org/10.3389/fncel.2020.555591.

[25] Ni M, Li J, Zhao H, Xu F, Cheng J, Yu M, *et al*. BRD4 inhibition sensitizes cervical cancer to radiotherapy by attenuating DNA repair. Oncogene. 2021; 40: 2711–2724. https://doi.org/10.1038/s41388-021-01735-3.

[26] Li J, Ma J, Meng G, Lin H, Wu S, Wang J, *et al*. BET bromodomain inhibition promotes neurogenesis while inhibiting gliogenesis in neural progenitor cells. Stem Cell Research. 2016; 17: 212–221. https://doi.org/10.1016/j.scr.2016.07.006.

[27] Puy L, Leboullenger C, Auger F, Bordet R, Cordonnier C, Bérézowski V. Intracerebral Hemorrhage-Induced Cognitive Impairment in Rats Is Associated With Brain Atrophy, Hypometabolism, and Network Dysconnectivity. Frontiers in Neuroscience. 2022; 16: 882996. https://doi.org/10.3389/fnins.2022.882996.

[28] Wang W, Wang R, Jiang Z, Li H, Zhu Z, Khalid A, *et al*. Inhibiting Brd4 alleviated PTSD-like behaviors and fear memory through regulating immediate early genes expression and neuroinflammation in rats. Journal of Neurochemistry. 2021; 158: 912–927. https://doi.org/10.1111/jnc.15439.

[29] Yang Z, He N, Zhou Q. Brd4 recruits P-TEFb to chromosomes at late mitosis to promote G1 gene expression and cell cycle progression. Molecular and Cellular Biology. 2008; 28: 967–976. https://doi.org/10.1128/MCB.01020-07.

[30] Zou M, Ke Q, Nie Q, Qi R, Zhu X, Liu W, *et al*. Inhibition of cGAS-STING by JQ1 alleviates oxidative stress-induced retina inflammation and degeneration. Cell Death and Differentiation. 2022; 29: 1816–1833. https://doi.org/10.1038/s41418-022-00967-4.

[31] Shi X, Bai H, Wang J, Wang J, Huang L, He M, *et al*. Behavioral Assessment of Sensory, Motor, Emotion, and Cognition in Rodent Models of Intracerebral Hemorrhage. Frontiers in Neurology. 2021; 12: 667511. https://doi.org/10.3389/fneur.2021.667511.

[32] Chen S, Peng J, Sherchan P, Ma Y, Xiang S, Yan F, *et al*. TREM2 activation attenuates neuroinflammation and neuronal apoptosis via PI3K/Akt pathway after intracerebral hemorrhage in mice. Journal of Neuroinflammation. 2020; 17: 168. https://doi.org/10.1186/s12974-020-01853-x.

[33] Xu W, Ocak U, Gao L, Tu S, Lenahan CJ, Zhang J, *et al*. Selective autophagy as a therapeutic target for neurological diseases. Cellular and Molecular Life Sciences. 2021; 78: 1369–1392. https://doi.org/10.1007/s00018-020-03667-9.

[34] Chen Zhou ZH, Salvador Álvarez E, Hilario Barrio A, Cárdenas Del Carre AM, Romero Coronado J, Ramos González A. Primary and secondary non-traumatic intra-cerebral haem-

orrhage: MRI findings. Radiologia. 2023; 65: 149–164. https://doi.org/10.1016/j.rxeng.2023.01.003.

[35] Gross BA, Jankowitz BT, Friedlander RM. Cerebral Intraparenchymal Hemorrhage: A Review. JAMA. 2019; 321: 1295–1303. https://doi.org/10.1001/jama.2019.2413.

[36] Qureshi AI, Mendelow AD, Hanley DF. Intracerebral haemorrhage. Lancet. 2009; 373: 1632–1644. https://doi.org/10.1016/S0140-6736(09)60371-8.

[37] Aronowski J, Zhao X. Molecular pathophysiology of cerebral hemorrhage: secondary brain injury. Stroke. 2011; 42: 1781–1786. https://doi.org/10.1161/STROKEAHA.110.596718.

[38] Wang X, Yu B, Cao B, Zhou J, Deng Y, Wang Z, *et al*. A chemical conjugation of JQ-1 and a TLR7 agonist induces tumoricidal effects in a murine model of melanoma via enhanced immunomodulation. International Journal of Cancer. 2021; 148: 437–447. https://doi.org/10.1002/ijc.33222.

[39] Zong D, Gu J, Cavalcante GC, Yao W, Zhang G, Wang S, *et al*. BRD4 Levels Determine the Response of Human Lung Cancer Cells to BET Degraders That Potently Induce Apoptosis through Suppression of Mcl-1. Cancer Research. 2020; 80: 2380–2393. https://doi.org/10.1158/0008-5472.CAN-19-3674.

[40] Xue J, Zhu Y, Bai S, He C, Du G, Zhang Y, *et al*. Nanoparticles with rough surface improve the therapeutic effect of photothermal immunotherapy against melanoma. Acta Pharmaceutica Sinica. B. 2022; 12: 2934–2949. https://doi.org/10.1016/j.apsb.2021.11.020.

[41] Honig LS, Rosenberg RN. Apoptosis and neurologic disease. The American Journal of Medicine. 2000; 108: 317–330. https://doi.org/10.1016/s0002-9343(00)00291-6.

[42] He L, Li H, Wu A, Peng Y, Shu G, Yin G. Functions of N6-methyladenosine and its role in cancer. Molecular Cancer. 2019; 18: 176. https://doi.org/10.1186/s12943-019-1109-9.

[43] Newton K, Strasser A, Kayagaki N, Dixit VM. Cell death. Cell. 2024; 187: 235–256. https://doi.org/10.1016/j.cell.2023.11.044.

[44] Li Y, Chen Y. AMPK and Autophagy. Advances in Experimental Medicine and Biology. 2019; 1206: 85–108. https://doi.org/10.1007/978-981-15-0602-4_4.

[45] Li X, Zhu R, Jiang H, Yin Q, Gu J, Chen J, *et al*. Autophagy enhanced by curcumin ameliorates inflammation in atherogenesis *via* the TFEB-P300-BRD4 axis. Acta Pharmaceutica Sinica. B. 2022; 12: 2280–2299. https://doi.org/10.1016/j.apsb.2021.12.014.

[46] Sakamaki JI, Wilkinson S, Hahn M, Tasdemir N, O'Prey J, Clark W, *et al*. Bromodomain Protein BRD4 Is a Transcriptional Repressor of Autophagy and Lysosomal Function. Molecular Cell. 2017; 66: 517–532.e9. https://doi.org/10.1016/j.molcel.2017.04.027.

[47] Campbell GR, Bruckman RS, Herns SD, Joshi S, Durden DL, Spector SA. Induction of autophagy by PI3K/MTOR and PI3K/MTOR/BRD4 inhibitors suppresses HIV-1 replication. The Journal of Biological Chemistry. 2018; 293: 5808–5820. https://doi.org/10.1074/jbc.RA118.002353.

[48] Hu CAA, White K, Torres S, Ishak MA, Sillerud L, Miao Y, *et al*. Apoptosis and autophagy: the Yin–Yang of homeostasis in cell death in cancer. In Hayat MA (ed.) Autophagy: Cancer, Other Pathologies, Inflammation, Immunity, Infection, and Aging (pp. 161–181). Academic Press: Amsterdam. 2015. https://doi.org/10.1016/B978-0-12-801043-3.00010-8.

[49] Chen Q, Kang J, Fu C. The independence of and associations among apoptosis, autophagy, and necrosis. Signal Transduction and Targeted Therapy. 2018; 3: 18. https://doi.org/10.1038/s41392-018-0018-5.